Journal of Intelligent & Fuzzy Systems 39 (2020) 53–68
DOI:10.3233/JIFS-190586
IOS Press

New hybrid SPEA/R-deep learning to predict optimization parameters of cascade FOPID controller according engine speed in powertrain mount system control of half-car dynamic model

Dinh-Nam Dao[a,b,*] and Li-Xin Guo[a,*]
[a]*School of Mechanical Engineering and Automation, Northeastern University, Shenyang, China*
[b]*Control Technology College, Le Quy Don Technical University, Hanoi, Viet Nam*

Abstract. In this article, a new methodology, hybrid genetic algorithm GA, algorithm SPEA/R with Deep Neural Network (HDNN&SPEA/R). This combination gave computing time much faster than computing time when using genetic algorithms SPEA/R. On the other hand, this combination also significantly reduces the number of samples needed for the training of deep artificial neural networks. This is the task of finding out an optimal set that changes with the engine velocity of multi-objective optimization involving 12 simultaneous optimization goals: proportional P, integral I, derivative D, additional integration n and differentiation orders m factor, displacement amplification coefficient K_{Dloop}, acceleration amplification coefficient K_{Aloop} in two controllers acceleration and displacement to enhance the ride comfort. This article has provided a control algorithm of a Cascade FOPID controller to control the acceleration and displacement of the mount. Besides, the article also offers solutions to optimize the 12 simultaneous parameters of the two controllers by the new hybrid method HDNN&SPEA/R and suitable for the speed of rotation of the engine. To increase the safety factor in operation, we use magnetorheological dampers (MR) in a powertrain mounting system and a continuous state damper controller that calculates the input voltage to the damper coil. The results of this control method are compared with traditional PID systems, optimal PID parameter adjustment using genetic algorithms (GA) and passive drive system mounts. The results are tested in both time and frequency domains, to verify the success of the proposed Cascade FOPID algorithm. The results show that the proposed Cascade FOPID controller of the MR engine mounting system gives very good results in comfort and softness when riding compared to other controllers. This proposal has reduced 335 hours for optimal computation time and reduce vibration a lot.

Keywords: SPEA/R algorithm, feed forward artificial neural network, magnetorheological MR, powertrain mounting system, FOPID controllers, PID controllers

1. Introduction

The problem of shaking in cars is one of the most important issues in Front Wheel Drive (FWD) cars. Therefore, we need to enhance the stiffness of the front body, the stiffness of steering support and the

*Corresponding author. Li-Xin Guo. E-mail: lxguo@mail.neu.edu.cn; Dinh-Nam Dao. E-mail: daodinhnambk@gmail.com.

Fig. 1. Test engine vibration according to the rotation speed of the engine.

floor stiffness on the body to reduce the vibration impact. On the engine side, we need to make flexible engine mounts to prevent the engine from falling off. Many studies are showing that when the engine operates at different rotational speeds, the vibration forces are different. Therefore, the design of the engine mounts must have the stiffness of the mount, which can flexibly change according to the vibration levels of different engines to always create a feeling of pleasure. On the other hand, two-speed ranges are of particular interest: low idling and the speed range of the loaded condition (1500 to 6000 RPM). At low engine speed range, idle vibration can be an important phenomenon because no-load speed can coincide with the natural frequency of the structure. Booming noise is another characteristic related to vibration stimulation and it usually occurs at high engine speeds. Resonance of the cavity is stimulated by the inertial force of the engine that causes explosive noise. Due to the interaction of the excitation and transfer path, it requires low vibration amplitude of the engine and high transmission loss in rubber mounts and vehicle structure. From the characteristics of the engine causing vibration during vehicle operation, we need to design the engine mount control system to have a flexible control mechanism according to the operation mechanism of the vehicle to achieve high efficiency in limiting vibrations arise on the whole operation of the vehicle. Thereby to bring comfort and softness for people when using cars.

From the features that are simple and easy to implement, the PID controller has been applied in various engineering applications and industries worldwide (Barbosa et al., [1]; Biswas et al., [2]; Jiang et al., [3]). Today, PID controllers are getting more and more interested by researchers to improve control performance. In addition to the FOPID or PI^nD^m controller, they have added two control parameters, n, and m (integrative and derivative orders), which are not being limited to integers that are fractions. This new controller was published by Podlubny [4]. The controller consists of five parameters: proportional, integral, derivative gains, the integral and derivative orders. The FOPID controller has superior performance and strength compared to the classical PID controller, and this has been demonstrated through the research articles mentioned previously. The FOPID controller has the advantage of denying steady-state error, robustness toward plant uncertainties and also good disturbance elimination. Vibration reduction and control are extremely suitable when using FOPID controllers (Aldair and Wang, [5]; Zhihuan et al., [6]). Aldair and Wang [5] have announced improvements to the FOPID controller. They have used evolution optimization algorithms to modulate control parameters and are applied in a full vehicle nonlinear active suspension of the car system. Hydraulic turbine regulating system was Zhihuan et al. [6] uses the FOPID controller that is optimized by a genetic algorithm that is not dominated by II.

Nowadays, From the requirements for easy execution, low power requirements, high power capacity, dynamic range and higher durability, the application of MR dampers is becoming popular in the semi-active Powertrain mounting system. Furthermore, the ability to supply the voltage/current needed to create a continuously variable damping force can be guaranteed on all modern vehicles today. Semi-active control devices use MR dampers with simple control requirements. It is only the voltage control lever applied to the electromagnetic coil that can be supplied directly. In addition to the system, the controller determines the damping force required for the system to achieve outstanding performance, a damping controller is required to calculate the voltage applied to the MR dampers.

Multi-objective evolutionary algorithms (MOEAs) are common tools for solving multi-objective optimization problems in the technical field, because of their performance on issues with large design spaces and scenes difficult exercise. Inside, SPEA2 (Intensity 2 Evolutionary Algorithm) is used to evaluate the Pareto solution due to the good performance of a variety of solutions different from normal multi-objective reliability assessment. There are some researchers in this field like Tommasi et al. [8] who have proposed a multi-objective optimization for RF circuit blocks through replacement models and NBI and SPEA2 methods. Sokratis Sofianopoulos [9] proposed a model-based machine translation system using large monolithic blocks in the target language from which statistical information was extracted.

This study reported using a specific machine translation to represent the test that SPEA2 was chosen as the optimization method. Zhao. F et al. [10] proposed a SPEA2 algorithm based on adaptive selection evolutionary operators (AOSPEA). The proposed algorithm can selectively adapt simulated binary interference, polynomial mutations, and differential evolutionary operators in their evolution according to their contribution to the external repository. IMEN et al. [11] proposed the Pareto Strength (SPEA2) Evolution Algorithm for the Economic / Environmental Power Distribution (EEPD) problem. In the past, minimizing fuel costs is the only objective function of economic power coordination. Due to the modification of clean air behavior has been applied to reduce emissions of polluting emissions from power plants, utilities have also changed strategies to reduce pollution and atmospheric emissions, minimizing generation Waste when other target functions turn economic capacity (EPD) into a versatile-objective problem with conflicting goals. Shouyong et al. [7] published a new SPEA based on the reference direction, denoted SPEA/R, to optimize multiple goals. a significant extension of the early SPEA algorithms is SPEA/R. It applies to the advantage of SPEA2's physical assignment in quantifying solutions Diversity and convergence in one method It is appropriate to replace the most time-consuming density estimator with an algorithm based on the reference direction. Their proposed exercise duties also take into account the convergence both local and global. However, MOEAs algorithms still need a lot of computational time to evaluate the objective function in the typical practical problem-solving process. When the problem is more difficult and complicated, the time to solve such problems requires many minutes or half an hour for an evaluation. Combined, this could make the use of MOEAs algorithms impractical. Therefore the best way to reduce computation time is to use artificial neural networks with multiple hidden layers plus deep learning algorithms to accelerate calculations.

The artificial neural network (ANNs) with hidden layers combined with deep learning algorithms is one of the most widely used and accurate predictive models. Many researchers have applied this method in areas such as economics, engineering, society, foreign exchange, securities issues, etc. [12–20]. The application of neural networks in predictive models optimizes many goals based on the ability of neural networks to predict non-fixed behavior is very accurate. For traditional mathematical models or statistical models, it is inconsistent with unusual data patterns that cannot be written as functions or deduced from a formula, while ANN algorithms can work with chaotic components. Currently, there are some researchers such as Yanxia Shen, Xu Wang, and Jie Chen [21], who have come up with potential uncertainties of wind power and have since proposed options for building intervals prediction (PI) with predictive models using wavelet neural network (WNN). In which the upper and lower limit estimate (LUBE) of PI has been implemented by minimizing the multi-objective function including the probability of span width and coverage range. Christopher Smith; John Doherty; Yaochu Jin [22], They announced a recurrent neural network used as an alternative method to predict long-term models of fluid dynamics simulation in computation. In particular, hybrid multi-objective evolutionary algorithms have been trained and optimized structures from introduced recurrent neural networks. Amir-Hasan Kakaee et al. [23], published a method of using artificial neural networks (ANN) followed by multi-objective optimization using the NSGA-II evolution algorithm and SPEA2 optimization algorithm to optimize the operating parameters of a compression ignition (CI) heavy-duty diesel engine. A Vieira and R S Tome [24], they published two different methods to increase the search speed of the multi-objective evolution algorithm (MOEA) using artificial neural networks. Duan, Lixiang, et al. [34] used deep learning to diagnose errors.

In this paper, a new hybrid optimization method is proposed for optimizing multi-objective problems. This is a combination of genetic algorithm (GA), Deep Neural Network (DNN) and Strength Pareto evolutionary algorithm based reference direction for Multi-objective (SPEA/R) to find the best of the Pareto-optimal front of Parameter of Cascade FOPID controllers according to the speed. This combination gave computing time much faster than computing time when using genetic algorithms SPEA/R. On the other hand, this combination also significantly reduces the number of samples needed for the training of deep artificial neural networks. Therefore it has facilitated and quickly in the application to find the optimal set of parameters of the Cascade FOPID controller, which is optimal according to the engine's rotation speed. This article has provided a control algorithm of the Cascade FOPID controller to control the acceleration and displacement of the mount through an optimize set of 12 simultaneous parameters of the two controllers to suitable for the speed of rotation of the engine. The results of this

control method are compared with traditional PID systems, optimal PID parameter adjustment using genetic algorithms (GA) and passive drive system mounts. The results are tested in both time and frequency domains, to verify the success of the proposed Cascade FOPID algorithm. The results show that the proposed Cascade FOPID controller of the MR engine mounting system gives very good results in comfort and softness when riding compared to other controllers.

The organization of this paper is as follows: Section 2 describes the proposed new hybrid HDNN&SPEA/R method and design Semi-active engine mount control system using MR dampers in a half-car dynamic model, formulation the objective functions for controller tuning, the proposed method of turning the Cascade FOPID controller use hybrid HDNN&SPEA/R method. Section 3 describes the Numerical simulation and results. Finally is a conclusion.

2. Structure

2.1. Many-objective optimization SPEA/R algorithm

Shouyong et al. (2017) proposed SPEA/R algorithm is presented in the flowchart of SPEA/R is shown in Fig. 2.

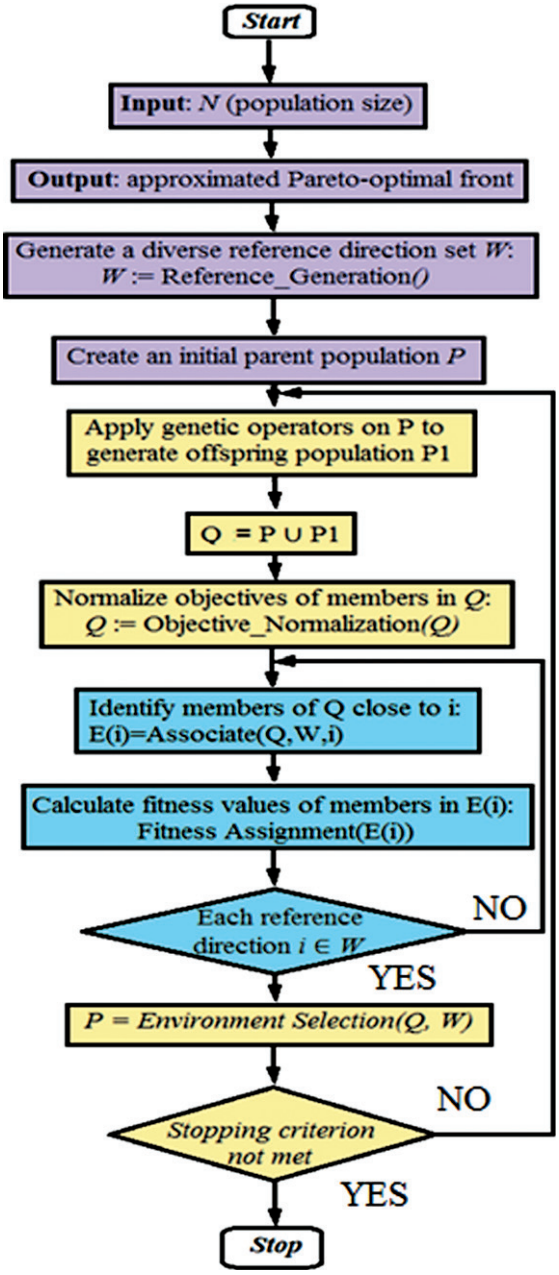

Fig. 2. Flowchart of SPEA/R.

2.2. New hybrid HDNN&SPEA/R method

2.2.1. Design a Deep Neural Network(DNN)

Artificial neural networks are simulations of simplified models of the human brain. They have the ability to estimate complex nonlinear relationships between corresponding input and output data parameters [23–27]. As shown in Fig. 3, the neural network has a link structure consisting of three types of classes. It is an input layer, hidden layer, and output layer. Each network layer consists of some neurons and is organized into layers. In which the nerve cells of different layers in the network are connected by connections connected to independent weights (W). Also, an independent bias (b) can be added to each neuron. On the other hand, the transfer function determines the influence of the weights and biases of the neuron on the neurons of the next layer and can be linear or nonlinear. Also, there are several types of transfer functions (such as pureline, logic, tansig), some neurons and some hidden layers are hyper-parameters of neural networks to create different structures of the network. neuron. Finally, weights and biases adjustment process are called the network training process and they are usually evaluated by minimizing the average square error (MSE) between the predicted outputs of the neural network and the output reality.

In this article, we use the (MLP) multilayer perceptron neural network structure. Network MLP is

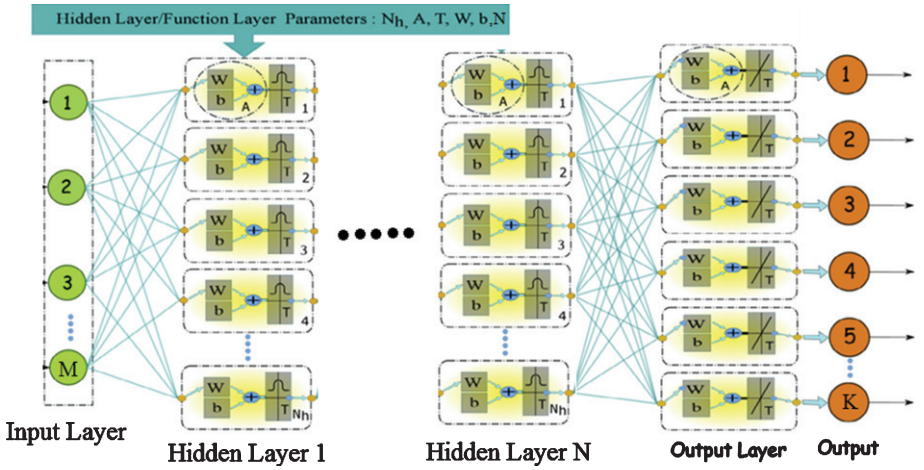

Fig. 3. The architecture of a feedforward artificial neural network with M neurons in input, N in hidden layer and K in output layers.

a feedforward artificial neural network defined by an input layer with M neurons. N layers hidden, in which each hidden layer has N_h number of neurons and an output layer has K neurons. In the MLP network structure, each layer has full connections to the next layer, which means that each neuron output in layer N is the input of each neuron in the $N + 1$ layer. Figure 2 shows one example of an MLP network with input neuron M, N hidden layer with each hidden layer has N_h neuron and the output layer has K neurons. MLP network can be described with: nn = [M N_{h1} N_{h2} ... N_{hN} K].

2.2.2. *DNN network optimize*

Recently, some researchers have published some new effective methods to train ANN neural networks. In which the weights and biases of neural networks are optimized by the GA algorithm [22]. In the process of network training, the GA algorithm finds weight and bias values quickly and optimally for neural networks. That makes the number of iterations in network training greatly reduced. Thus, the time for training is faster. Besides, the global ability of searching and the evolution of parameters is a key feature of GA. Therefore, the GA algorithm was introduced in this study. This method uses the theory of natural selection and biological evolution. It is the choice, cross-exchange, and mutation of individuals to select the best and most suitable member. The initial weight and bias of the DNN network have been evolved in the process of training neural networks. The interaction between the GA algorithm and the DNN network is done through weight and bias exchange. The DNN network was started to get a random weight and biases [W, b] as shown in Fig. 3. This is the initial population included in the GA algorithm. Then, the next generation is generated by the GA algorithm based on the current population. To evaluate the difference between the predicted output values and the actual output values, it is used as the fitness function. Decide on acceptable parameters if the total average square of GA is less than 0.005. Weight and biases are calculated by the equations (1)

$$N_w = (I_n + 1)N_h + (N_h + 1)O_p \tag{1}$$

Where N_w is a number of weights and deviations, I_n is a number of neurons in the input layer, N_h is some hidden neurons and an O_p number of neurons in the output layer. Through the training process, the optimal GA value has been achieved. Algorithm GA with population size is 20, the mutation rate is 0.15 and the crossover rate is 0.65 has been chosen for GA operation. GA algorithm has been run for 250 generations.

2.2.3. *The deep learning training algorithm*

Let the DNN neural network learn the optimal analytical characteristics of many objects from the SPEA/R algorithm. We have combined DNN training with the optimal analysis of the SPEA/R algorithm as shown in Figs. 4 and 5. This process started with the SPEA/R algorithm with a random population of input variables P_1. After that, summing up the population Q at time t is created by population P_1 and population P_2 (where P_2 is generated from P_1 parents' population through the use of conventional genetic operators such as selection, mutations and cross exchanges). After that, all individuals were combined into populations Q. From this population,

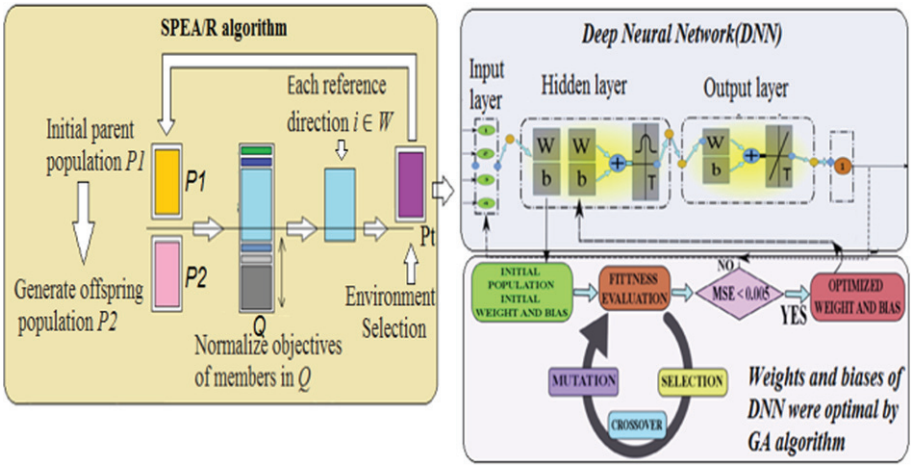

Fig. 4. Training structure for the hybrid method.

Algorithm 1
Training DNN network optimize

1:Input: Pareto temporary front set
2: Output: weight and bias values optimized
3: Initializing parameters
Population size
Number of generation
Probabilities of selection
Crossover and mutation
Fitness function
Mean square error
4: Creating initial population parent encoding weight and bias
5: **while** *stopping criterion not met* **do**
6: Calculation fitness
7: Evolution of population
8: Fitness ranking
9: Selection crossover
10: Selection of fitness and update
11: Record the best chromosome
12: **end while**

individuals were selected to enhance reproduction instead of random selection. It is therefore very useful for optimizing many goals when remote parents are unable to create good solutions. The use of simple normalization based on the worst value of each SPEA/R goal deliberately gives higher priority to diversity than convergence when making environmental choices leading to printing performance for MOP issues. From there, the best Pareto fronts were selected (stored on the top of the list) and transferred to the new parent group P_t. Through this process, the most quintessential nuclei were selected. Since the size of the P_t population is only half of Q (in fact the size of P_t is equal to the size of P_1) so half of the Pareto front will be deleted during the transfer. This process will be continued until all individuals of a specific Pareto front cannot be completely provided in the parent population of P_t. Therefore, for choosing the exact number of individuals of that particular front for filling remained space of the population P_t, an associate population with reference points to keep a constant number of individuals (POP: population size). Finally, the population update process P_t will be used to replace population P_1 in the next generation of the SPEA/R algorithm and the Pareto temporary front optimization will be defined after a specific generation can. Therefore, after each cycle of population update ($P_{t)}$ in the SPEA/R algorithm, Pareto temporarily will be transferred to the DNN network including input data and output data (that is the Temporary Pareto front) to train the DNN network. From here, we see a lot of Temporary Parero font files created from the SPEA/R algorithm, which means there are many standard data sets for training DNN networks. Therefore, the combined training of the DNN network has the full characteristics of the SPEA/R algorithm, but it has a fast calculation speed and converges faster of neural networks. The search area is larger than the SPEA/R algorithm because the DNN network is trained on many standard samples.

Thus, through this deep learning training, the artificial neural network has learned all the characteristics of the Many-objective optimization SPEA / R algorithm. But due to the characteristic of the neural network working in parallel and at the same time in the neurons, the calculation speed to find the optimal parameters is much faster than the SPEA / R algorithm. SPEA / R is the process of performing calculations through the loop cycle, so that the calculation process takes a lot of time when the number of

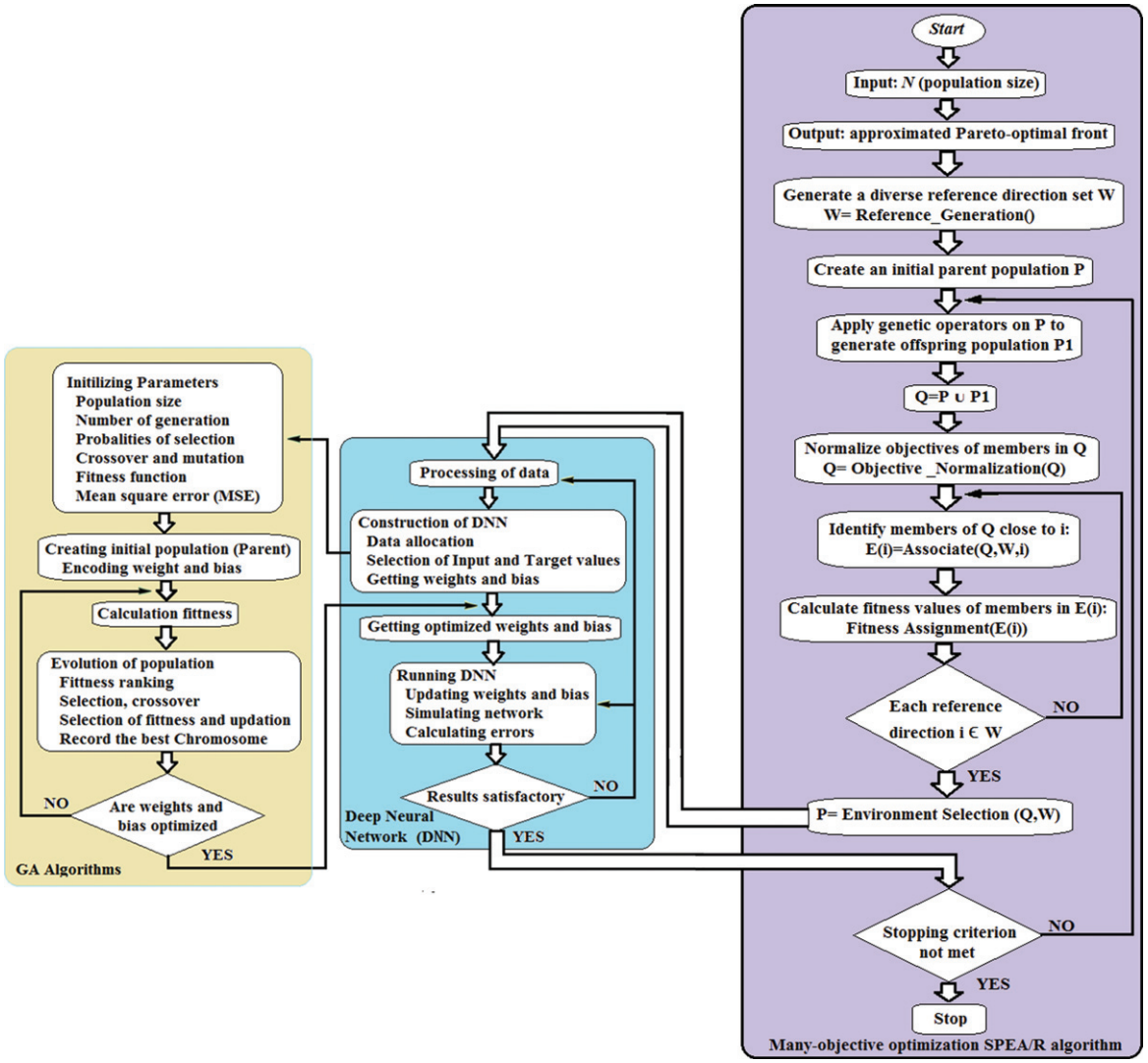

Fig. 5. Training algorithm.

iterations increases. Thus, this deep learning method has created a deep neural network capable of finding optimal parameters quickly.

2.2.4. *Leave one out cross-validation (LOOCV) method*

Cross-validation is the most common and effective way to verify models in statistical machine learning. This method is intended to estimate predictive models that they have learned from training data. How it will do on data that has not been tested in the future. In other words, by this method, we can measure the generalized power (accuracy) of our trained model in practice and avoid overfitting when the use of techniques cross-validation. Leave-one-out cross-validation (LOOCV) is the most common cross-authentication method. This technique is often applied when the amount of training and testing data is not too large or too difficult to create a large training/test data set for model learning. With this method, in each iteration, a sample of the temporary data point is considered the validation data and the remaining data is used for model training. Through each model training process, its prediction errors will be calculated on the validation data. If the initial training data contains Iter_max samples, this procedure repeats Iter_max times (it equals the number of observations in the initial training set). Then, the average of

Algorithm 2
Training DNN network

1: **Input**: *N* (population size)
2: **Output**: Pareto-optimal front set
3: Create a diverse set of reference directions *F*:
F: = Reference Create ();
4: Create an original parent population *P1*
5: **while** *stop criterion not met* **do**
6: Apply this genetic operator *P1* to create offspring
7: *Q:* = *P1* ∪ *P2*;
8: Normalize the goals of internal members *Q*:
Q: = Objective normalization*(Q)*
9: **for** each reference direction $i \in F$ **do**
10: Identify members of *Q* close to *i*:
H(i) : = Associate*(Q, F, i)*;
11: Perform calculations fitness values of members in
H(i): Fitness assignment*(H(i))*
12: **end for**
13: P_t: = Choose the environment*(Q, F)*
14: Call Algorithm 1
15: **end while**

these errors is reported as the predictive error of our predictive model across the entire data set in terms of expressions by equations (2). Thus, with this validation method, in its iterations Iter_max, all patterns have the opportunity to act as a prototype. For more information on LOOCV, refer to [24].

$$\sum_{\text{error}} = \left(\sum_{i=1}^{Iter\_max} |Iter_{-i}| \right) / Iter_{-max} \qquad (2)$$

2.3. Design semi-active engine mount control system using MR dampers in a half-car dynamic model

2.3.1. A mathematical model of the semi-active engine mount control system in a half-car dynamic model

The mounts play an important role in the car dynamics system. The principle diagram of the semi-active engine mount control model with the transmission system is shown in Fig. 6.

By using Newton's law, the mathematical model of Fig. 6 can be written as below:

$$\mathbf{M}\ddot{\mathbf{x}}_\mathbf{i} + \mathbf{K}\dot{\mathbf{x}}_\mathbf{i} + \mathbf{C}\mathbf{x}_\mathbf{i} = \mathbf{Q}(t) \qquad (3)$$

In which:

$\mathbf{x_i}$: Vector-column of displacements and angular oscillations of masses.

M: Matrix of inertial coefficients of car parts.

C: Matrix of coefficients of stiffnesses and torsional rigidity.

K: Matrix of damping coefficients.

Q(t): Column vector of the perturbing forces and moments.

$q_2(t) = q_1(t + \tau)$ with τ: time interval, va vehicle speed.

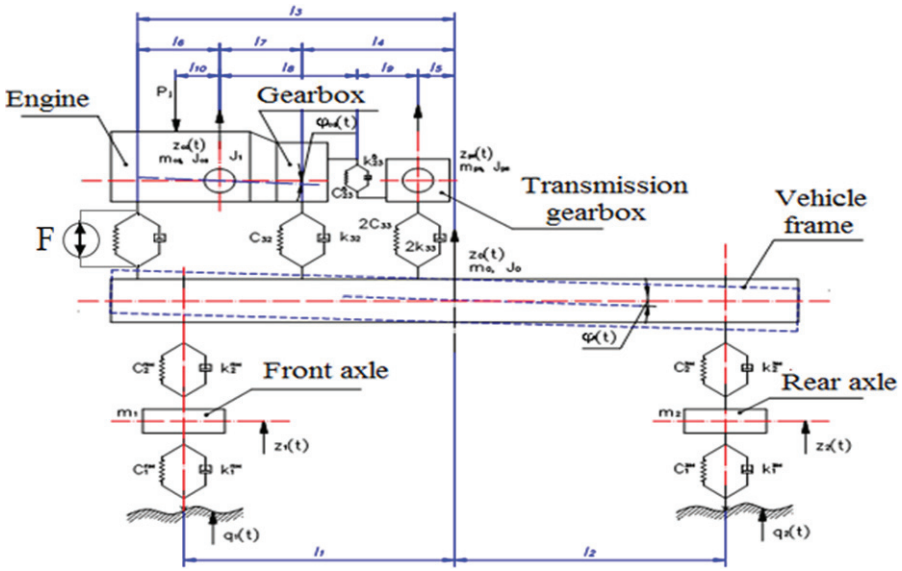

Fig. 6. Half-car dynamic model with a semi-active engine mount.

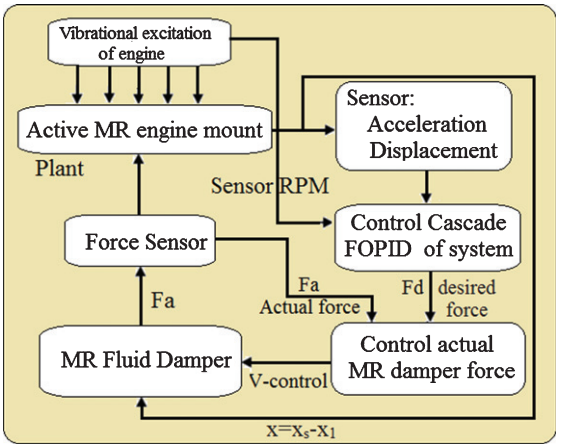

Fig. 7. Control system structure of semi-active MR engine mount.

$$\mathbf{Q}(t) = \begin{bmatrix} 2k_1^{\Pi M}\cdot\dot{q}_1(t) + 2C_1^{\Pi M}\cdot q_1(t), 2k_2^{\Pi M}\cdot\dot{q}_2(t) + \\ 2C_2^{\Pi M}\cdot q_2(t), 0, 0, P_j(t), P_j(t)\cdot l_{10}, F\cdot l_6, 0, 0, \\ M(t), 0, 0, 0, 0, \gamma\cdot\left[2\cdot k_1^{\Pi M}\cdot\dot{q}_1(t) + 2\cdot C_1^{\Pi M}\cdot q_1(t)\right], \\ \gamma\cdot\left[2\cdot k_2^{\Pi M}\cdot\dot{q}_2(t) + 2\cdot C_2^{\Pi M}\cdot q_2(t)\right], 0, 0, 0 \end{bmatrix}^T \quad (4)$$

$$X = \begin{bmatrix} z_1, z_2, z_0, \varphi_0^{y}, z_{ca}, \varphi_{ca}^{y}, z_{pk}, \varphi_{ca}^{x}, \varphi_{pk}^{x}, \\ \varphi_1, \varphi_2, \varphi_3, \varphi_4, \varphi_5, \varphi_6, \varphi_7, \varphi_8, \varphi_{\Pi M}, \varphi_{3M} \end{bmatrix}^T \quad (5)$$

2.3.2. *Design semi-active engine mount control system*

This control system consists of two controllers which are Cascade FOPID controllers and damping controllers. In which the Cascade controller consists of two closed control loops to control the acceleration and displacement of the mount for calculation desirable damping force Fd. The damping controller receives the control request from the Fd Cascade FOPID controller, thus calculating the voltage V applied to the damping coil and always monitoring its actual force Fa with the desired Fd force to make the decision suitable controller. The entire semi-active engine mount system incorporating the MR damper process described in Fig. 7.

2.3.3. *Actual MR damper controller*

Sims et al., [28] published a continuous state control (CSC) algorithm. They applied this algorithm in the model of an ER damper. Next, some researchers (for example, Metered et al., [29]; Gad et al., [30]) also gave an algorithm to calculate the voltage command applied to the male MR Damper coil.

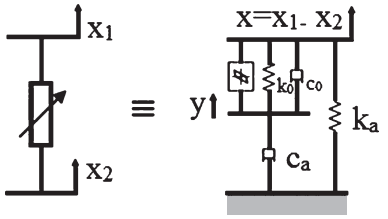

Fig. 8. Modified Bouc-Wen model.

Table 1
Parameters of Modified Bouc-Wen model (Lai and Liao, [31])

Parameter	Value	Parameter	Value
c_{oa}	784 Nsm^{-1}	α_a	12441 Nm^{-1}
c_{ob}	1803 $NsV^{-1}m^{-1}$	α_b	38430 $NV^{-1}m^{-1}$
k_o	3610 Nm^{-1}	γ	136320 m^{-2}
c_{aa}	14649 Nsm^{-1}	β	2059020 m^{-2}
c_{ab}	34622 $NsV^{-1}m^{-1}$	δ	58
k_a	840 N m^{-1}	n	2
x_o	0.0245 m	η	190 s^{-1}

It allows the command voltage V to change continuously between the minimum and maximum values 0, V_{max} according to the following equation.

$$v = \begin{cases} 0; G(F_d - LF_d)\,\mathrm{sgn}(F_d) < 0 \\ G(F_d - LF_a)\,\mathrm{sgn}(F_a); 0 \le G(F_d - LF_d) \\ \quad \mathrm{sgn}(F_d) \le V_{\max} \\ V_{\max}; G(F_d - LF_d)\,\mathrm{sgn}(F_d) > V_{\max} \end{cases} \quad (6)$$

(F_d-LF_d) is the error signal. with L is the feedback gain. CSC is only activated when the error and the damping force are the same sign. With the maximum voltage is V_{max} and the minimum voltage is V_{min}, the desired damping force is F_d and the actual MR damper force is F_a, the scaled gain is G.

The historical time elements of the voltage applied to the coil from V and the relative displacement x on the dampers are parameters that affect the damping force MR of the semi-active engine mount system (x is the distance to move the mount).

$$x = x_s - x_1 \quad (7)$$

Lai and Liao [31] improved the Bouc - Wen model as shown in Fig. 8 to calculate the actual MR damping force. By solving the modified Bouc - Wen model of this MR damper based equations from 8 to 14, we obtained the given signals V and x, the Fa force, and the parameters listed in Table 1.

$$F_a = c_a\,\dot{y} + k_a(x - x_0) \quad (8)$$

$$\dot{y} = \frac{1}{c_0 + c_a}\left\{\alpha z + c_0\,\dot{x} + k_0(x - y)\right\} \quad (9)$$

$$\dot{z} = -\gamma \left|\dot{x} - \dot{y}\right| \left|z|^{n-1} z - \beta(\dot{x} - \dot{y})\right| z|^2 + \delta(\dot{x} - \dot{y}) \quad (10)$$

$$\alpha = \alpha(u) = \alpha_a + \alpha_b u... \quad (11)$$

$$c_a = c_a(u) = c_{aa} + c_{ab} u... \quad (12)$$

$$c_0 = c_0(u) = c_{0a} + c_{0b} u... \quad (13)$$

$$\dot{u} = -\eta(u - v)... \quad (14)$$

y is Internal displacement of MR liquid damper.

u is an output of the first order filter.

v is Voltage command sent to the current driver.

ka is Hardness accumulated

ca is viscous shock absorbers observed at high speeds.

C0 is viscous shock absorbers observed at low velocities.

k0 is Control hardness at high speed.

The effect of the accumulator is calculated by x0.

expand the values for the modified Bouc–Wen model.

g, c, b, and A: The elements are used to adjust the ratio/shape of the delay ring.

2.3.4. *FOPID controller structure*

As the introduction says the advantages of the FOPID controller. The structure of the FOPID controller is shown in Fig. 9. This is the most common structure of the FOPID controller, it is $PI^n D^m$ involving integrator of order n and a differentiator of order m where n and m can be any real number. The transfer function of the controller shown as Laplace transform as follows:

$$G_c = K_p + K_i \frac{1}{s^n} + K_d s^m (m \text{ and } n > 0) \quad (15)$$

The five unknown gains in the optimization problem are n and m, along with K_p, K_i, and K_d that provide more possibility to recognize the optimum control performance. In addition, the error signal is a relative shift between the engine mount and chassis.

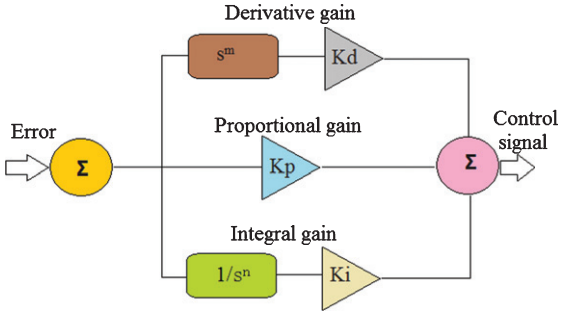

Fig. 9. FOPID controller structure.

In equation (15), when we set n and m equal to 1, we transferred the FOPID controller to the PID controller form. Similarly, set n to 1 and m to 0, we get the normal PI controller. Set n to 0 and m to 1 we get the normal PD controller. This can be further in-depth in designing the FOPID controller in the frequency domain published by (Das et al., [32]).

2.3.5. *Design of the cascade FOPID controller*

We provide the cascade FOPID control method as shown in Fig. 10. For the controller to meet the design requirements such as creating a sense of comfort and safety for humans when sudden acceleration and deceleration, the bumps of the road surface cause. Thus the controller needs to eliminate disturbances from the outside. On the other hand, relatively large stiffness is also needed to eliminate inertial disturbances caused by experimental loads. Therefore, to achieve very high control quality with strict response requirements of the required micro load of test load (Li et al., [33]), the FOPID controller with single-loop will be difficult to achieve. From that requirement, we designed the cascade FOPID controller with two closed loops that are controlled consecutively to control stability and simultaneously both the displacement and acceleration parameters of engine mount to vibration isolation. If the payload generates any disturbing acceleration then the accelerometer controls the corresponding force and matches the

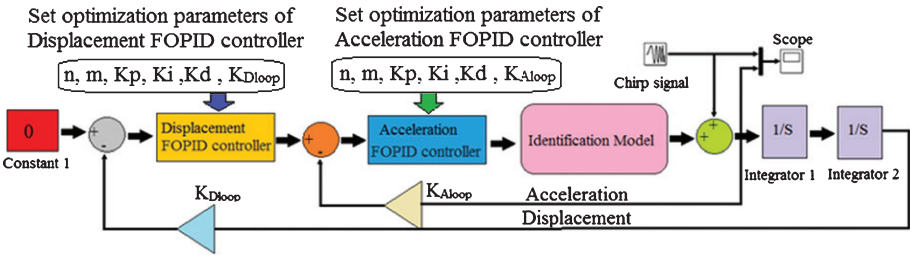

Fig. 10. Schematic diagram of the cascade FOPID control system.

false signal to counteract inertial motion. The float can float due to its acceleration. The main function of the main controller is to adjust the settings of the secondary circuit through its outer ring to change the initial acceleration; on the other hand, the function of the secondary controller (or accelerator controller) is to receive the output of the main controller and perform the corresponding regulation according to the accelerometer measurements to ensure acceleration. Loads can monitor various settings and timely adjustments can be made according to the movement of the buoy, and its displacement eventually returns to its center. For the Cascade FOPID controller to work perfectly, the most difficult thing is to calibrate the parameters of the two accelerator and displacement controllers simultaneously. Here we suggest using HDNN&SPEA/R hybrid algorithm to optimize these parameters according to the different rotation speed ranges of the engine so that there is the most optimal parameter set that meets the most sudden and harsh changes in the operation of the vehicle.

2.3.6. *Formulation the objective functions for controller tuning*

In this paper, the multi-objective optimization problem needs to be solved in order to find the optimal set of parameters (n, m, K_p, K_i, K_d, K_{Dloop}) of Displacement FOPID controller and (n, m, K_p, K_i, K_d, K_{Aloop}) of Acceleration FOPID controller based on the following objective functions. The objective of the object functions and the constraints to create a feeling of comfort and softness possible for humans. With ω_{cg} is gain crossover frequency, and Φ_m is phase margin. These two parameters selected as the two objectives for the optimization problem of the FOPID controller.

$$Maximize\ J_1 = w_{cg}\ and\ Maximize\ J_2 = \Phi_m \tag{16}$$

Through equation (16), we see, this is a condition to ensure the stability of the system when it is controlled under the FOPID controller. Next is equation (17) and (18) are the gain cross over frequency and phase margin of the controlled system respectively.

$$20\log\left|C(jw_{cg})G(jw_{cg})\right| = 0\ dB \tag{17}$$

$$Arg(C(jw_{cg})G(jw_{cg})) = -\pi + \Phi_m \tag{18}$$

Thus, for equation (16) is to maximize the ride comfort and efficiency of the controller the control system to operate very fast when ω_{cg} is very high value. To implement the optimization algorithm to maximize the goals in equation (16), a set of constraints has been combined for search with only solutions that bring positive and phase margins to bring good system stability. Their limitations and purposes are defined as follows:

1) If closed-loop transfer function has a small magnitude at a specified frequency ω to be less than specified gain H then it will reject the high-frequency noise as defined in the equation (19).

$$\frac{C(jw)G(jw)}{1 + C(jw)G(jw)_{dB}} \le H \tag{19}$$

2) Perform the fractional integrator of the order $k + \lambda, k \in N,\ 0 < \lambda < 1$ to eliminate the steady state error.
3) Two functions are extremely important, it directly affects the feeling of the human, that is the mean square acceleration (MSA), and mean square displacement (MSD) of the powertrain mount system is the smallest.
4) Equation (20) has performed the function of removing high frequencies from the system. This is significant because it ensures the robustness of the system

$$\frac{1}{1 + C(jw)G(jw)_{dB}} \le N \tag{20}$$

2.3.7. *Method of turning the cascade FOPID controller*

As mentioned in the introduction, during the operation of the vehicle, the engine causes unwanted effects. It vibrates to the chassis. Therefore, it makes the tired feeling uncomfortable for passengers. These unwanted vibrations vary with the speed of the engine's rotation. When the car is fast or slow, vibration is different. This process is completely random and nonlinear, it is difficult to control. Therefore, this paper has proposed a solution to the design control system with two closed feedback loops using 2 FOPID controllers combined with an optimal control parameter set according to the change of speed engine.

2.3.8. *Build the optimal parameter set for the adaptive control system according to the engine speed*

Cascade FOPID controller consists of two acceleration and displacements controllers. So for the Cascade FOPID controller to work well, it is neces-

sary to optimize the parameters of the two controllers. From the object functions and the constraints, we need to find the data set (n, m, K_p, K_i, K_d, K_{Aloop}) of acceleration controllers and data set (n, m, K_p, K_i, K_d, K_{Dloop}) of displacements controllers is optimal. We suggest using a hybrid HDNN&SPEA/R algorithm to save time on simulation calculations. Here, we used artificial neural networks with 4 hidden layers. This neural network is trained to learn deeply based on SPEA/R gene algorithm. Thus, this neural network has the same function as the SPEA/R gene algorithm but with higher accuracy and faster calculation time many times. In order to match the vehicle's performance characteristics such as sudden acceleration and deceleration and the controller's processing time, we have divided the engine rotation speed range (700RPM-6000 RPM) into 500 revolutions in each level. At each level, the HDNN&SPEA/R algorithm will be used to find the optimal set of parameters for the control system. Thus, the comfort and safety of the ride have been significantly enhanced. The Algorithm diagram calculates the optimal coefficients varying according to engine speed to be included in the cascade FOPID controller as shown in Fig. 11.

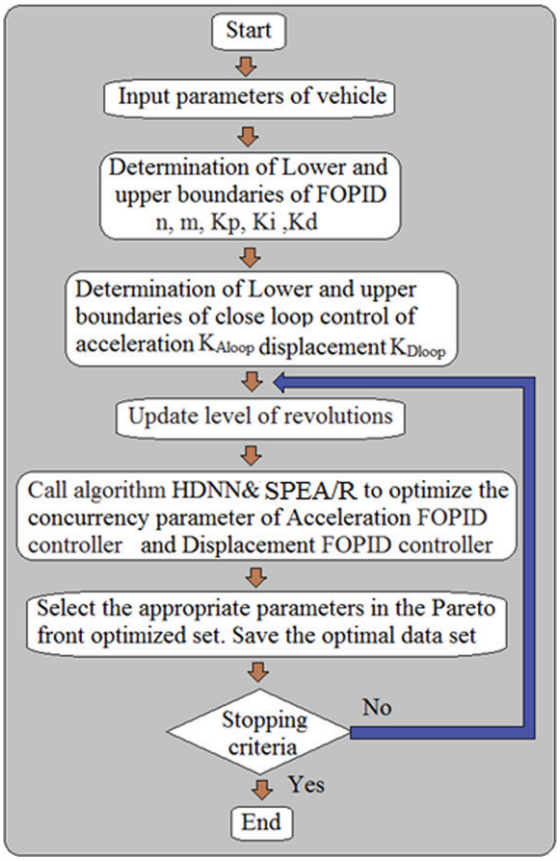

Fig. 11. Flow chart of an optimal parameter of cascade FOPID controller.

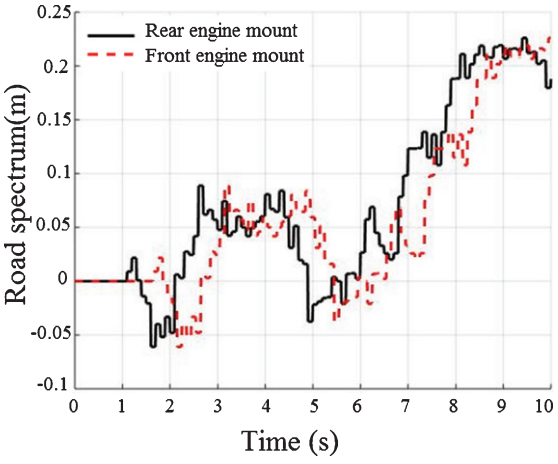

Fig. 12. Road surface profiles.

3. Numerical simulation and results

3.1. Simulated input parameters of the vehicle

Road surface profiles: When the vehicle moves many factors cause the vibration, the factors can be told: The internal force in the car; External forces appear in the process of using acceleration, braking, revolving; Exterior conditions such as wind and storm; boring face street. Among the factors on the

Table 2
Geometric parameters of engine (m)

l_1	l_2	l_3	l_4	l_5
1,225	1,175	1,330	0,520	0,190
l_6	l_7,	l_8	l_9	l_{10}
0,187	0,623	0,760	0,210	0,030

Table 3
General settings information of vehicle

Mass of the equipped automobile, m_0, kg	1210
Payload, kg	400
The weight of the front wheels, m_1, kg	37
The weight of the rear wheels, m_2, kg	37
The weight of the power unit, m_{ca}, kg	152,2
Transfer Case Weight, m_{pk}, kg	27,8
Radius crank, r, M	0,04
The ratio of the crank radius to the length of the connecting rod, λ	0,308
Wheel radius in slave mode, r_k, M	0,325

Table 4
Model parameters of SPEA/R algorithm and DNN network

Maximum number of iterations	Iter_max = 1000
Population Size	100
Crossover percentage	0.5
Mutation percentage	0.5
DNN network parameters	nn = [100 200 200 200 200 100]
Mutation rate = 0.02	0.02
Number of parnets (offsprings)	2*round (pCrossover*nPop/2)
Number of mutants	round (pMutation*nPop)
Mutation step size	0.1*(VarMax-VarMin)
Generating reference points	nDivision=10 Zr = GenerateReference Points(nObj, nDivision);

bumpy side of the road is the oscillation cause of the vehicle. To simulate the most general calculation, we use the road surface profile as a random function as in Fig. 12, and simulated parameters as shown in Tables 2–4.

Table 5
Set of optimal parameter cascade FOPID controller

Revolutions	Acceleration FOPID controller					
level(RPM)	n	m	K_p	K_i	K_d	K_{Dloop}
700–1200	0.73	0.45	71522.8	21455.2	4122.1	1.66
1200–1700	0.66	0.29	61341.3	30465.8	3827.5	1.84
1700–2200	0.65	0.37	51563.6	41556.4	4252.7	2.35
2200–2700	**0.72**	**0.59**	**42563.3**	**31351.3**	**5262.2**	**1.33**
2700–3200	0.75	0.53	55522.5	29405.3	6103.4	4.69
3200–3700	0.55	0.47	78542.9	51710.9	5332.7	1.50
3700–4200	0.58	0.36	61724.1	60938.1	7062.8	5.68
4200–4700	0.82	0.45	58520.2	51732.9	5162.3	6.45
4700–5200	0.78	0.25	76555.7	44450.6	6020.0	5.67
5700–6000	0.95	0.46	81614.8	70154.8	7139.3	2.85

Revolutions	Displacement FOPID controller					
level(RPM)	n	m	K_p	K_i	K_d	K_{Dloop}
700–1200	0.78	0.35	66555.7	45450.6	6220.0	4.78
1200–1700	0.77	0.57	62725.1	67928.1	7072.8	2.07
1700–2200	0.39	0.78	61352.3	30065.8	3429.5	5.37
2200–2700	**0.46**	**0.45**	**57563.6**	**45586.4**	**4257.7**	**3.35**
2700–3200	0.77	0.65	79562.8	27495.2	4162.1	5.78
3200–3700	0.63	0.82	61644.8	77150.8	7239.3	6.80
3700–4200	0.85	0.46	53570.2	53782.9	5662.3	2.64
4200–4700	0.45	0.55	45572.5	39475.3	6173.4	7.44
4700–5200	0.58	0.38	77512.9	57799.7	5432.7	4.64
5700–6000	0.52	0.56	42362.3	41380.3	5862.2	3.84

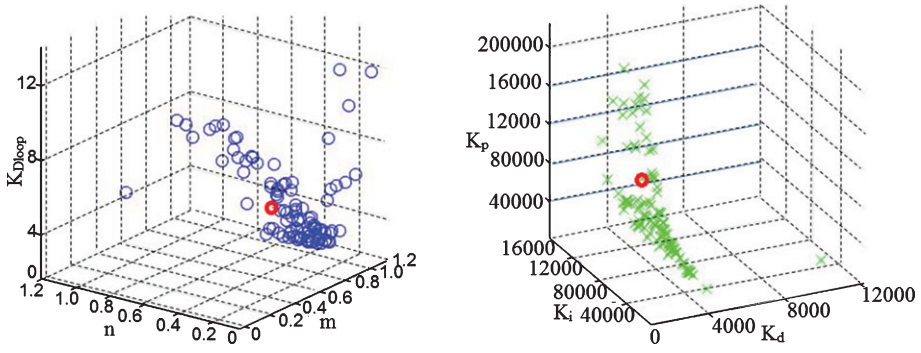

Parameters optimized of Acceleration FOPID controller

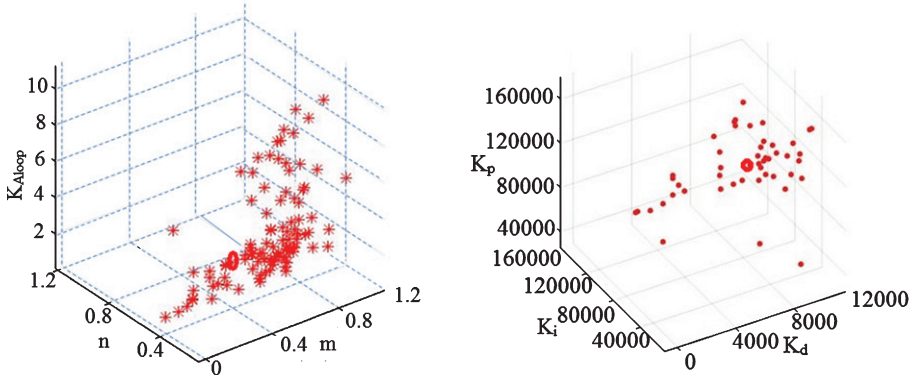

Parameters optimized of Displacement FOPID controller

Fig. 13. Parameters optimized of Acceleration, Displacement FOPID controller at speed range of 2200-2700(RPM).

4. Results

Through Matlab software to simulate, we have selected the optimal data set for the Cascade FOPID controller as shown in Table 5. Simulation analysis is performed in this section to evaluate the ride comfort.

In Fig. 13. (shows the results in the form of 4D, 4-dimensional space via the Isosurfaces function in Matlab) is the result of a case of a rotation speed range at 2200-2700(RPM) as shown in Table 5. In the figure, the Pareto optimization front is set according to the parameters of accelerator and displacement controllers. Based on the need to rejuvenate comfort and softness, we have selected the values that correspond to the mean square acceleration (MSA), and mean square displacement (MSD) of the powertrain mount system is the smallest in this Pareto front set (Those are the red circles with the bold net).

In Fig. 14 is the result of a case of a rotation speed range at 2200-2700(RPM). The black points in the figure show the results of calculating the acceleration and displacement values of the MR engine mount corresponding to the stiffness values of the mount to be controlled. This value is given by the Cascade FOPID controller to Control the actual MR damper force.

In Figs. 15–18, symbol A corresponds to the passive drive system mounts, B is traditional PID systems, C is optimal PID parameter adjustment using genetic algorithms (GA), D is Cascade FOPID controller.

In Figs. 15 and 16. With the Cascade FOPID controller, we see that the acceleration and displacement of the chassis are the smallest and it is much smaller than the results of the remaining controllers. Thus, the Cascade FOPID controller has superior advantages compared to other controllers. It has eliminated high-frequency noise, preventing the sudden acceleration and deceleration of the vehicle.

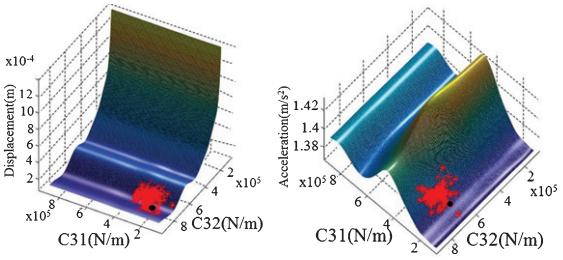

Pareto front of MSD at the front engine mount.

Pareto front of MSA at the front engine mount

Fig. 14. Global Pareto front of MSD, MSA front engine mount.

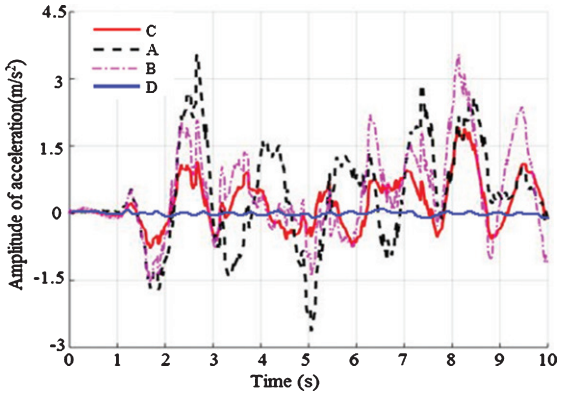

Fig. 15. Acceleration of the vehicle frame.

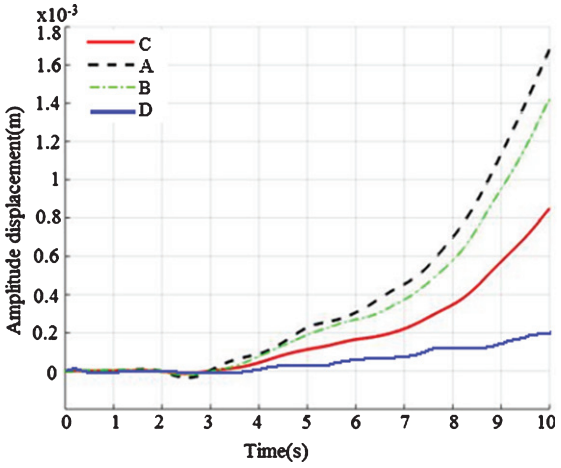

Fig. 16. Displacement of the vehicle frame.

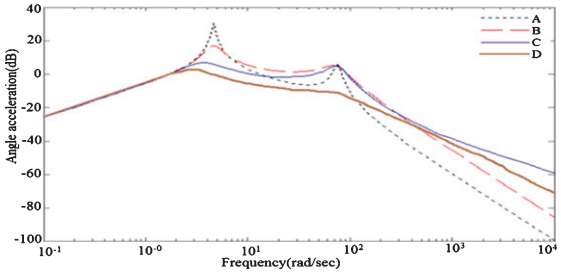

Fig. 17. Respond by frequency.

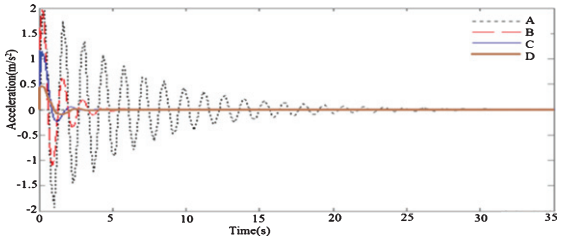

Fig. 18. Respond by time.

Based on the simulation results in the frequency domain as shown in Fig. 17 at both resonance points, the Cascade FOPID controller achieves lower oscillation transmission than the other three systems. Therefore the system achieves better performance, creating a feeling of comfort and smooth ride softer. Simulated in the time domain as shown in Fig. 18, Cascade FOPID controller has the smallest oscillation amplitude, also the shortest damping time. Thus the Cascade FOPID controller has demonstrated optimal control over the other three controllers. It has brought more comfort to people.

5. Conclusion

This paper has published a new combination method between SPEA/R, DNN, and GA. So artificial neural networks with many hidden layers are trained with intelligent deep learning algorithms, it has created a deep learning network to realize the optimal problem simultaneously of many objects in the technology. This method is extremely effective and highly practical because: Firstly, it offers a way of deep learning of the network with a much smaller number of standard samples than previous deep-learning networking methods announced. For test cases Optimal parameter Cascade FOPID controller, we only need a standard set of 10 samples to train deep neural networks. It is this combination of training that the actual number of samples generated for the training process is $10 \times (\text{Iter\_max}) = 10000$ samples. While training with the old method is extremely difficult to collect a large number of samples. Secondly, for test cases, Optimal parameter Cascade FOPID controller, the time for multi-objective optimal analysis of HDNN&SPEA/R hybrid methods at 1 Revolutions level(RPM) is only 1.5 hours while using SPEA/R algorithm takes 35 hours. So the total time for calculating the entire process for the optimal controller will be $(35\text{-}1.5) \times 10 = 335$ hours.

Thus, This article has published the Cascade FOPID controller and control algorithms. This controller has an optimal set of control parameters that adapt to the changing of the speed range of the engine rotation. The Cascade FOPID controller has been designed successfully. It has demonstrated superior advantages over previous controllers. On the other hand, it has met the requirements set out to prevent vibrations during a sudden increase or decrease of the engine when the engine changes different rotation speeds, from which it creates a comfortable feeling. roof, soft when riding for people. This is completely proven in the simulation results.

Acknowledgment

This work was supported by the National Natural Science Foundation of China (51875096, 51275082).

Conflict of interest

None.

References

[1] R.S. Barbosa, J.A.T. Machado and I.S. Jesus, Fractional PID control of an experimental servo system, *Computers & Mathematics with Applications* **59** (2010), 1679–1686.

[2] A. Biswas, S. Das, A. Abraham and S. Dasgupta, Design of fractional-order PID controllers with an improved differential evolution, *Engineering Applications of Artificial Intelligence* **22** (2009), 343–350.

[3] C. Jiang, Y. Ma and C. Wang, PID controller parameters optimization of hydroturbine governing systems using deterministic-chaotic-mutation evolutionary programming (DCMEP), *Energy Convers Manage* **47** (2006), 1222–1230.

[4] I. Podlubny, Fractional-Order Systems and PID Controllers, *IEEE Transaction on Automatic Control* **44** (1999), 208–214.

[5] A.A. Aldair and J.W. Wang, Design of fractional order controller based on evolutionary algorithm for a full vehicle nonlinear active suspension systems, *International Journal of Control and Automation* **3** (2010), 33–46.

[6] C. Zhihuan, Y. Xiaohui, J. Bin, W. Pengtao and T. Hao, Design of a fractional order PID controller for hydraulic turbine regulating system using chaotic non-dominated sorting genetic algorithm II, *Energy Convers Manage* **84** (2014), 390–404.

[7] S. Jiang and S. Yang, Senior Member, A Strength Pareto Evolutionary Algorithm Based on Reference Direction for Multiobjective and Many-Objective Optimization, *IEEE Transactions On Evolutionary Computation* **21**(3) (2017).

[8] L. De Tommasi, T.G.J. Beelen, M.F. Sevat, J. Rommes and E.J.W. Maten, ter, Multi-objective optimization of RF circuit blocks via surrogate models and NBI and SPEA2 methods in CASA-report Eindhoven 2011: *Technische Universiteit Eindhoven* **1132** (2011).

[9] S. Sofianopoulos and G. Tambouratzis, Studying the SPEA2 Algorithm for Optimising a Pattern-Recognition Based Machine Translation System', *Proceedings of the 2011 IEEE Symposium on Computational Intelligence in Multicriteria Decision-Making (MCDM 2011)*, 11–15 (2011), 97–104. Paris, France, In Proceedings.

[10] F. Zhao, W. Lei, W. Ma, Y. Liu and C. Zhang, An improved SPEA2 algorithm with adaptive selection of evolutionary operators scheme for multiobjective optimization problems, *Mathematical Problems in Engineering*, **2016** (2016), Article ID 8010346, 20 pages.

[11] I.B. Hamida, S.B. Salah, F. Msahli and F.M. Mouhamed, Strength Pareto Evolutionary Algorithm 2 For Environmental/Economic Power Dispatch', in *ICMIC 2015:7th International Conference on Modelling, Identification, and Control*, (2015), Tunisia - December 18–20.

[12] M. Shakouri Hassanabadi and S. Banihashemi, Developing an empirical predictive energy-rating model for windows by using Artificial Neural Network, *Int J Green Energy* (2012).

[13] K. Hansen, et al., Machine learning predictions of molecular properties: Accurate many-body potentials and nonlocality in chemical space, *Te J Phys Chem Lett* **6** (2015), 2326–2331.

[14] G. Montavon, et al., Learning invariant representations of molecules for atomization energy prediction, In F. Pereira, C.J.C. Burges, L. Bottou and K.Q. Weinberger, (eds.) *Advances in Neural Information Processing Systems* **25** (2012), 440–448 (Curran Associates, Inc.).

[15] K.Y. Chan, T. Dillon, E. Chang and J. Singh, Prediction of short-term traffic variables using intelligent swarm-based neural networks, *IEEE Transactions on Control Systems Technology* **21**(1) (2013), 263–274. https://doi.org/10.1109/tcst.2011.2180386.

[16] M.V. Leelavathi and S.D. KJ An architecture of deep learning method to predict traffic flow in big data, *International Journal of Research in Engineering and Technology* **05**(16) (2016), 461–468. https://doi.org/10.15623/ijret.2016.0516100.

[17] W. Huang, G. Song, H. Hong and K. Xie, Deep architecture for traffic flow prediction: deep belief networks with multitask learning, *IEEE Trans Intell Transport Syst* **15**(5) (2014), 2191–2201.

[18] J. Wang, J. Wang, W. Fang and H. Niu, Financial time series prediction using elman recurrent random neural networks, *Computational Intelligence and Neuroscience* (2016), Article ID 4742515, 14 pages.

[19] J. Sreekanth and B. Datta, Multi-objective management of saltwater intrusion in coastal aquifers using genetic programming and modular neural network based surrogate models, *Journal of Hydrology* **393**(3-4) (2010), 245–256.

[20] G. Lesinski and S. Corns, Multi-objective Evolutionary Neural Network to Predict Graduation Success at the United States Military Academy, *Complex Adaptive Systems Conference with Theme: Cyber Physical Systems and Deep Learning*, CAS (2018), 5 November–7 November 2018, Chicago, Illinois, USA.

[21] Y. Shen*, X. Wang and J. Chen, Wind Power Forecasting Using Multi-Objective Evolutionary Algorithms for Wavelet Neural Network-Optimized Prediction Intervals, Published: 26 January 2018, *Appl Sci* **8** (2018), 185. doi:10.3390/app8020185, www.mdpi.com/journal/applsci.

[22] C. Smith, J. Doherty and Y. Jin, Multi-objective evolutionary recurrent neural network ensemble for prediction of computational fluid dynamic simulations, Beijing, China 6–11 July 2014v : 2014 *IEEE Congress on Evolutionary Computation (CEC)* DOI: 10.1109/CEC.2014.6900552

[23] A.-H. Kakaee, P. Rahnama and A. Paykani, Combining artificial neural network and multi-objective optimization to reduce a heavy-duty diesel engine emissions and fuel consumption, *Journal of Central South University* **22**(11) (2015), 4235.

[24] A. Vieira and R.S. Tome, A Multi-Objective Evolutionary Algorithm Using Neural Networks To Approximate Fitness, *International Journal of Computers, Systems and Signals* **6**(1) (2005), 18–36.

[25] I.N. Tansel, S. Gulmez, M. Demetgul and S. Aykut, Taguchi Method– GONNS integration: Complete procedure covering from experimental design to complex optimization, *Expert Systems with Applications* **38** (2010), 4780–4789.

[26] A.C.P. Filho and R.M. Filho, Hybrid training approach for artificial neural networks using genetic algorithms for rate of reaction estimation: Application to industrial methanol oxidation to formaldehyde on silver catalyst, *Chemical Engineering Science* **157** (2010), 501–508.

[27] K. Ron, A study of cross-validation and bootstrap for accuracy estimation and model selection, *1995 Proceedings of the Fourteenth International Joint Conference on Artificial Intelligence*, 1137–1143.

[28] N.D. Sims, R. Stanway, D.J. Peel and W.A. Bullough, Controllable viscous damping: an experimental study of an electrorheological long-stroke damper under proportional feedback control, *Journal of Smart Materials and Structures* **8** (1999), 601–615.

[29] H. Metered, P. Bonello and S.O. Oyadiji, An investigation into the use of neural networks for the semi-active control of a magnetorheologically damped vehicle suspension, In: *Proceedings of the Institution of Mechanical Engineers, Part D: Automobile Engineering* **224** (2010), 829–848.

[30] S. Gad, H. Metered, A. Bassuiny and A.M. Abdel Ghany, Ride Comfort Enhancement of Heavy Vehicles using Magnetorheological Seat Suspension, *International Journal of Heavy Vehicle System* **22** (2015), 93–113.

[31] C.Y. Lai and H.W. Liao, Vibration Control of a Suspension System via a Magnetorheological Fluid Damper, *Journal of Vibration and Control* **8** (2002), 527–547.

[32] S. Das, S. Saha, S. Das and A. Gupta, On the selection of tuning methodology of FOPID controllers for the control of higher order processes, *ISA Trans* **50** (2011), 376–388.

[33] Y. Li, J. Liu, Z. Yang, et al., Dynamics and control of a parallel mechanism for active vibration isolation in space station, *Nonlinear Dynamics* **76**(3) (2014), 1737–1751.

[34] L. Duan, et al., Deep learning enabled intelligent fault diagnosis: Overview and applications, *Journal of Intelligent & Fuzzy Systems* **35**(5) (2018), 5771–5784. DOI: 10.3233/JIFS-17938.